Spatially controlled bond formation has been realized with the STM. The fact that the CO ligand exhibits an inclined configuration in the Fe-Ag(110) system suggests that the observed geometry is due to the localized electronic properties of the Fe atom. In contrast, it would be interesting to determine if a single CO molecule would bond perpendicularly, without tilting or bending, with a different metal atom, such as Cu, on Ag(110) (*23*).

The binding of a diatomic molecule to an atom constitutes one of the simplest chemical transformations involving a molecule. By combining the present manipulation approach with other mechanisms such as "sliding" (*1*), "pulling," and "pushing" (*3*, *4*), extension of spatially controlled bond formation to other atoms and molecules is envisioned. The ability to control step-by-step bond formation of adsorbed chemical species at the single-molecule level provides a real-space understanding and direct visualization of the nature of the chemical bond. An important function of STM-IETS lies in the confirmation and identification of the new bonds formed.

References and Notes

1. D. M. Eigler and E. K. Schweizer, *Nature* **344**, 524 (1990).
2. M. F. Crommie, C. P. Lutz, D. M. Eigler, *Science* **262**, 218 (1993).
3. L. Bartels, G. Meyer, K.-H. Rieder, *Phys. Rev. Lett.* **79**, 697 (1997).
4. J. K. Gimzewski and C. Joachim, *Science* **283**, 1683 (1999).
5. B. J. McIntyre, M. Salmeron, G. A. Somorjai, *Science* **265**, 1415 (1994).
6. B. C. Stipe, M. A. Rezaei, W. Ho, *Phys. Rev. Lett.* **81**, 1263 (1998).
7. ———, *Science* **280**, 1732 (1998).
8. ———, *Phys. Rev. Lett.* **82**, 1724 (1999).
9. B. C. Stipe *et al.*, *Phys. Rev. Lett.* **78**, 4410 (1997).
10. G. Dujardin, R. E. Walkup, Ph. Avouris, *Science* **255**, 1232 (1992).
11. The STM is a variation of the one described by B. C. Stipe, M. A. Rezaei, and W. Ho [*Rev. Sci. Instrum.* **70**, 137 (1999)].
12. Sample bias voltages greater than 2.4 V and tunneling currents of a few nanoamperes were used to transfer CO between the Cu(111) surface and the tip [L. Bartels *et al.*, *Phys. Rev. Lett.* **80**, 2004 (1998)].
13. The Fe(CO) can also be formed by pushing the CO with the tip toward the Fe atom at a sample bias of <70 mV and tunneling current of 10 nA. This process, however, is less controlled because the direction of motion of the CO is not predictable; the CO does not always follow the tip trajectory.
14. W. Erley, *J. Vac. Sci. Technol.* **18**, 472 (1981).
15. K. Tanaka, Y. Tachikawa, T. Tanaka, *Chem. Phys. Lett.* **281**, 285 (1997).
16. R. Fournier, *J. Chem. Phys.* **99**, 1801 (1993).
17. S. Hirota *et al.*, *J. Phys. Chem.* **98**, 6652 (1994).
18. On Ag(110), CO moves when it is scanned at 0.25 V and 1 nA, making it difficult to probe the C–O stretch by STM-IETS. However, the CO hindered rotation mode has been observed at 19 meV without causing the molecule to move. The C–O stretch is observed at 261 meV by high-resolution electron energy loss spectroscopy [R. A. Pelak and W. Ho, *Surf. Sci.* **321**, L233 (1994)].
19. The presence of the CO molecule on the tip is verified by changes in the STM topographical images (Fig. 2D versus Fig. 4E). Additional evidence is obtained by positioning the tip over a clean area on the Ag(110) surface and observing by STM-IETS two vibrational peaks: the hindered rotation at 19 meV and the C–O stretch at 267 meV for $^{12}C^{16}O$ and 253 meV for $^{13}C^{18}O$. These energies are close to those of CO on Ag(110) (*18*), suggesting that the tungsten tip is terminated with Ag because of physical contacts made with the surface during in situ tip conditioning.
20. O. González-Blanco and V. Branchadell, *J. Chem. Phys.* **110**, 778 (1999).
21. D. W. Moon, D. J. Dwyer, S. L. Bernasek, *Surf. Sci.* **163**, 215 (1985).
22. U. Burghaus and H. Conrad, *Surf. Sci.* **331-333**, 116 (1995).
23. A single CO molecule adsorbs vertically on an atop site through the carbon atom on both Cu(001) and Cu(110) surfaces as determined by STM-IETS [L. J. Lauhon and W. Ho, *Phys. Rev. B* **60**, R8525 (1999)].

24. Supported by the Department of Energy, Basic Energy Sciences grant DE-FG02-91ER14205.

10 August 1999; accepted 26 October 1999

Mechanical Rotation of the c Subunit Oligomer in ATP Synthase (F_0F_1): Direct Observation

Yoshihiro Sambongi,[1] Yuko Iko,[1] Mikio Tanabe,[1] Hiroshi Omote,[1]* Atsuko Iwamoto-Kihara,[2] Ikuo Ueda,[1] Toshio Yanagida,[3] Yoh Wada,[1] Masamitsu Futai[1]†

F_0F_1, found in mitochondria or bacterial membranes, synthesizes adenosine 5′-triphosphate (ATP) coupling with an electrochemical proton gradient and also reversibly hydrolyzes ATP to form the gradient. An actin filament connected to a c subunit oligomer of F_0 was able to rotate by using the energy of ATP hydrolysis. The rotary torque produced by the c subunit oligomer reached about 40 piconewton-nanometers, which is similar to that generated by the γ subunit in the F_1 motor. These results suggest that the γ and c subunits rotate together during ATP hydrolysis and synthesis. Thus, coupled rotation may be essential for energy coupling between proton transport through F_0 and ATP hydrolysis or synthesis in F_1.

The proton-transporting ATP synthase, F_0F_1, consists of a catalytic sector, F_1 or F_1–adenosine triphosphatase (ATPase) ($\alpha_3\beta_3\gamma_1\delta_1\varepsilon_1$), and a proton pathway, F_0 ($a_1b_2c_{12}$) (*1*, *2*). The crystal structure of the bovine $\alpha_3\beta_3\gamma$ complex indicates that the α and β subunits are arranged alternately around the NH_2- and COOH-terminal α helices of the γ subunit (*3*). The isolated F_1 hydrolyzes ATP, followed by γ subunit rotation, which is driven by conformational changes of the catalytic subunits (*4*). The γ subunit rotation in F_1 has been suggested by biochemical experiments (*5*) and has been observed directly as counterclockwise rotation of an actin filament connected to the γ subunit (*6*, *7*).

The γ subunit rotation in F_1 should be transmitted to the membrane sector, F_0, in order to complete the ATP hydrolysis–dependent proton transport. The detailed underlying mechanism of the energy transmission between F_0 and the γ subunit remains unknown. If the c subunit oligomer rotates counterclockwise (the same direction as γ) in the membrane, the ATP hydrolysis–dependent γ subunit rotation could be connected mechanically to the F_0 sector. In this regard, c subunit rotation has been proposed (*2*, *8*). However, to the best of our knowledge, this possibility of energy coupling has not been studied.

We designed several experimental systems to examine this possibility. The γ and ε complex is shown to be a rotor (*6–9*) and the α, β, δ, a, and b complex is proposed to be a stator in F_0F_1 (*8*). Therefore, we fixed F_1 α (or β) subunits on a glass surface to demonstrate the rotation of an actin filament connected to the F_0 c subunit, or conversely, the c subunits were fixed and the rotation of α or β was examined. ATP-dependent rotation was only successfully observed with the system described below (*10*). *Escherichia coli* F_0F_1 was immobilized on a coverslip through a His tag linked to the NH_2-terminus of each α subunit (Fig. 1). A c subunit Glu^2 was replaced by cysteine and then biotinylated to bind streptavidin and a fluorescently labeled actin filament. The γ subunit cysteine residues were replaced with alanine (*11*) in order to avoid direct binding of the actin filament to this subunit. Thus, cysteine is present only in the c subunit of the presumed rotor complex of the

[1]Division of Biological Sciences, Institute of Scientific and Industrial Research, Osaka University, CREST (Core Research for Evolutional Science and Technology) of Japan Science and Technology Corporation, Ibaraki, Osaka 567–0047, Japan. [2]Department of Biology, Graduate School of Arts and Sciences, University of Tokyo, Komaba, Tokyo 153–8902, Japan. [3]Department of Physiology, Osaka University Medical School, Suita, Osaka 565–0871, Japan.

*Present address: Department of Molecular Physiology and Biological Physics, University of Virginia, Charlottesville, VA 22906–0011, USA.

†To whom correspondence should be addressed. E-mail: m-futai@sanken.osaka-u.ac.jp

engineered F_0F_1. Specific biotinylation of the c subunit in F_0F_1 was confirmed by protein immunoblotting with streptavidin (*12*).

After the addition of Mg ATP (*13*), the actin filament that was connected to the c subunit rotated. This rotation required Triton X-100 (*14*). Similar to the γ subunit in the F_1 sector, the c subunit rotated counterclockwise when viewed from the membrane side (*15*). Nuclear magnetic resonance structure and biochemical or genetic analyses suggested that 12 copies of the c subunit form a symmetrical cylinder in which the NH_2-terminus including Glu^2 faces the periplasmic surface of the central pore of ~1 nm in diameter (*16*). Therefore, the actin filament may be connected in the vicinity of the central pore.

Video images of the filaments connected to the c subunits were processed through centroid analysis (*13*); thus, the time course of the rotation could be obtained (Fig. 2A). Filaments connected to the c subunit continued to rotate for up to 2 min after the addition of Mg ATP, whereas filaments connected to the γ subunit in F_1 often rotated for more than 10 min (*7, 12*). The filaments connected to the c subunits ceased rotations abruptly and disappeared from the glass surface in all cases, possibly because of the dissociation of the F_0 sector from the F_1 sector.

The rotational rates varied slightly during the video recording, when the scales for the rotation and assay time were expanded (see Fig. 3A, upper left trace, for an example). The rates of single molecules were obtained, and the average values with deviations were plotted against the filament length (Fig. 2B). The results indicate that the c subunit rotation generates an average frictional torque of 40 pN·nm, which is similar to the value obtained for the γ subunit in F_1 (*7*). Thus, mechanical energy transmission from the γ subunit to the c oligomer occurs essentially with no energy loss.

We examined whether venturicidin, an *E. coli* membrane F_0F_1 inhibitor (*17*), could affect the c subunit rotation. After the addition of the antibiotic, the rotations frequently paused and started again on a subsecond scale (Fig. 3A, upper traces). In contrast, the γ subunit rotation in F_1 remained unchanged (Fig. 3A, lower traces). The effects of venturicidin on the rotations of c and γ subunits were statistically analyzed by counting the number of pauses (*18*). In the c subunit rotation, the pauses after the venturicidin addition increased fivefold in comparison with those before the addition, whereas the antibiotic had no effect on the γ subunit rotation (Fig. 3B). The inhibitory effect on the c subunit rotation was dependent on the concentration (*19*) (Fig. 3B), indicating that the antibiotic must be binding and then dissociating from the c subunit oligomer. These results are consistent with a previous suggestion that venturicidin binding sites are located around c subunit Asp^{61}

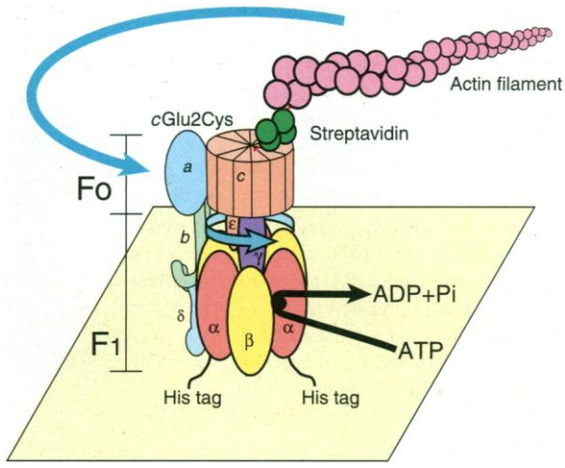

Fig. 1. Observation system for the c subunit rotation in F_0F_1 established in this study. The fluorescently labeled actin filament–biotin-streptavidin complex was connected to the cysteine residue introduced at position 2 of the c subunit. In this system, all cysteine residues in the γ subunit were replaced by alanine, and the ε subunit does not contain cysteine. Therefore, an actin filament cannot bind to the γ and ε subunits, which form a rotor with the c subunit (shown in this study). cGlu2Cys, $cGlu^2 \rightarrow Cys^2$.

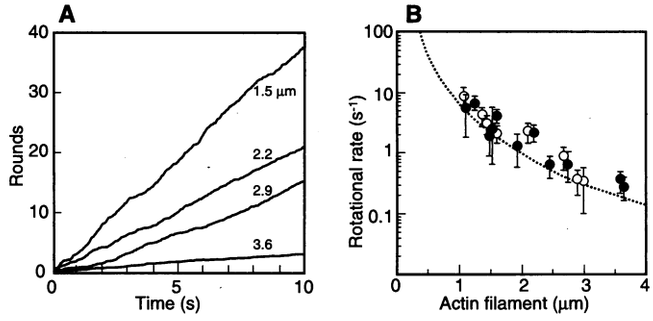

Fig. 2. Effects of actin filament length on the rotation of a filament connected to the c subunit. (**A**) The rotations (rounds) of actin filaments (1.5, 2.2, 2.9, and 3.6 μm) were recorded in the presence of 5 mM Mg ATP. (**B**) Rotational rate versus length of the actin filament. Rotating filaments connected to the c subunit at one end were analyzed. Linear segments having R^2 values of >0.96, except those defined as pauses (*18*), were selected from traces with an expanded time scale (examples shown in Fig. 3A), and then rotational rates were calculated. The average values for the rotational rates (~20 data points) are plotted with standard deviations (error bars) against filament length (solid circles). Frictional torque T was calculated with $T = (4\pi/3)\omega\eta L^3/[\ln(L/2r) - 0.447]$, where ω is angular velocity; η is 10^{-3} N·s m^{-2}, the viscosity of the medium; L is the length of the actin filament; and r is 5 nm, the radius of the actin filament (*24*). The dotted line represents the calculated rotational rates of the filaments with a constant torque value of 40 pN·nm. For comparison, the rotational rates of the γ subunit in F_1 are plotted (open circles). For the assay, 5 mM Mg ATP was used.

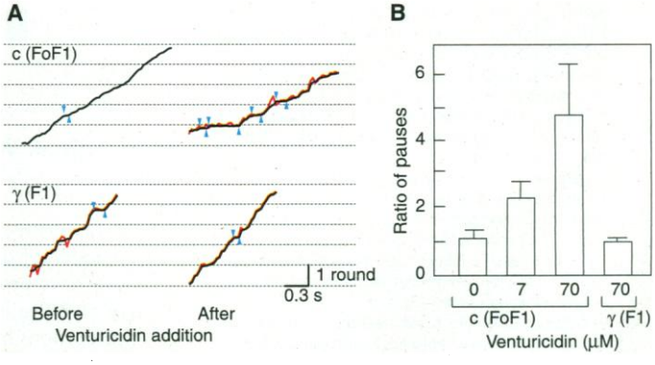

Fig. 3. Effect of venturicidin on the rotation of an actin filament connected to the c subunit of F_0F_1. Rotational movements of filaments were followed on a subsecond scale. During video recording for the rotating filaments, 20 μl of the reaction mixture containing 70 μM venturicidin (provided by R. H. Fillingame) was slowly (~5 μl/s) introduced into the flow cell, and the movement was further recorded. The approximate volume of the flow cell was 10 μl. (**A**) Typical examples of the rotations before (left trace) and 2 s after (right trace) the addition of venturicidin. Upper traces indicate the filament (2.0 μm) connected to the c subunit [$c(F_0F_1)$], and lower traces indicate the filament (1.6 μm) connected to the γ subunit [$\gamma(F_1)$]. Red lines show records obtained at a resolution of 33 ms; black lines show the same records passed through a nonlinear median filter of rank 5 (133-ms width) (*25*). Arrowheads (blue) pointing down and up indicate the beginning and end of pauses, respectively. (**B**) Increase of pauses after venturicidin addition. The rotations of five actin filaments (~1.5 to ~2.0 μm) connected to the F_0F_1 c or F_1 γ subunit were recorded, and numbers of pauses (per rotation, or round) after and before the venturicidin addition were counted. Ratios of the event numbers (pauses after venturicidin/pauses before venturicidin) and final venturicidin concentrations (0, 7, and 70 μM) are shown. Error bars indicate standard deviations.

(*E. coli*), which is essential for proton transport (*20*).

Our results indicate that the c subunit oligomer rotates with the γ subunit during ATP hydrolysis by F_0F_1. In the reverse direction, proton transport should drive rotation of the c subunit oligomer, which in turn would drive rotation of the γ subunit to promote ATP synthesis. Our study demonstrates that the mechanical rotation of the γ and c subunit complex is an essential feature for the energy coupling between proton transport through the F_0 sector and ATP hydrolysis or synthesis in the F_1 sector. Analysis of a series of *E. coli* F_0F_1 mutants (*21*), based on the progress of single molecule biomechanics (*22*), will contribute to the further understanding of the motor mechanism.

References and Notes

1. M. Futai, T. Noumi, M. Maeda, *Annu. Rev. Biochem.* **58**, 111 (1989); M. Futai and H. Omote, in *Handbook of Biological Physics, Volume 2*, W. N. Konings, H. R. Kaback, J. S. Lolkema, Eds. (Elsevier, Amsterdam, 1996), pp. 47–74; J. Weber and A. E. Senior, *Biochim. Biophys. Acta* **1319**, 19 (1997); R. H. Fillingame, *Curr. Opin. Struct. Biol.* **6**, 491 (1996); H. S. Penefsky and R. L. Cross, *Adv. Enzymol. Relat. Areas Mol. Biol.* **64**, 173 (1991).
2. P. D. Boyer, *Annu. Rev. Biochem.* **66**, 717 (1997).
3. J. P. Abrahams, A. G. W. Leslie, R. Lutter, J. E. Walker, *Nature* **370**, 621 (1994).
4. H. Wang and G. Oster, *Nature* **396**, 279 (1998).
5. R. Aggeler, M. A. Haughton, R. A. Capaldi, *J. Biol. Chem.* **270**, 9185 (1995); T. M. Duncan, V. V. Bulygin, Y. Zhou, M. L. Hutcheon, R. L. Cross, *Proc. Natl. Acad. Sci. U.S.A.* **92**, 10964 (1995).
6. H. Noji, R. Yasuda, M. Yoshida, K. Kinoshita Jr., *Nature* **386**, 299 (1997).
7. H. Omote *et al.*, *Proc. Natl. Acad. Sci. U.S.A.* **96**, 7780 (1999).
8. S. B. Vik and B. J. Antonio, *J. Biol. Chem.* **269**, 30364 (1994); W. Junge, H. Lill, S. Engelbrecht, *Trends Biochem. Sci.* **22**, 420 (1997); T. Elston, H. Wang, G. Oster, *Nature* **391**, 510 (1998); P. Dimroth, H. Wang, M. Grabe, G. Oster, *Proc. Natl. Acad. Sci. U.S.A.* **96**, 4924 (1999).
9. Y. Kato-Yamada, H. Noji, R. Yasuda, K. Kinoshita Jr., M. Yoshida, *J. Biol. Chem.* **273**, 19375 (1998).
10. The engineered *E. coli* F_0F_1 (αHis tag/cGlu^2 → Cys^2/γCys^{87} → Ala^{87}/γCys^{112} → Ala^{112}) was purified as described (*23*). The enzyme was treated with 100 μM 6-{*N*′-[2-(*N*-maleimido)ethyl]-*N*-piperazinylamido} hexyl D-biotinamide (Dojindo, Kumamoto, Japan) for 1 hour at 4°C. Specific biotinylation of the c subunit was confirmed by protein immunoblotting with streptavidin conjugated with alkaline phosphatase (Novagen, Madison, WI). This engineered F_0F_1 was used for rotation assay throughout our study. Fluorescently labeled biotinylated actin filaments were prepared as described (*7*). We also tested an engineered F_0F_1 (cGlu^2 → Cys^2) fused with biotin binding protein at the NH_2-terminus of the α subunit to bind the streptavidin-actin complex. The F_0F_1 was fixed through c subunit Cys^2 on beads coated with *N*-succinimidyl 4-maleimidobutyrate (Dojindo). This system produced no rotating filament.
11. Two cysteine residues (Cys^{87} and Cys^{112}) present in the γ subunit were replaced by site-directed mutagenesis that was based on polymerase chain reaction (*7*).
12. Y. Sambongi *et al.*, data not shown.
13. The engineered enzyme was immobilized by the slightly modified method previously described (*7*). Buffer A was included in all solutions used, unless otherwise specified, and was composed of the following: 10 mM Hepes-NaOH (pH 7.8), 25 mM KCl, 6 mM $MgCl_2$, bovine serum albumin (BSA) (10 mg/ml), and 0.24 mM Triton X-100. Ni–nitrilotriacetic acid horseradish peroxidase conjugate (0.8 μM) (Qiagen, Valencia, CA) in buffer A (without BSA and Triton X-100), 10 nM F_0F_1, and 4 μM streptavidin were successively introduced into the flow cell. Fluorescently labeled actin filaments (12.5 nM) were added to construct F_0F_1 with an attached actin filament, and finally, the reaction mixture for rotation [5 mM Mg ATP, 1 μM biotin, pyruvate kinase (50 μg/ml), 1 mM phosphoenol pyruvate, 25 mM glucose, 1% β-mercaptoethanol, glucose oxidase (216 μg/ml), and catalase (36 μg/ml) in buffer A] was introduced. The rotation was observed at 20°C with a Zeiss Axiovert 135 equipped with an intensified charge-coupled device camera (Atto Instruments, Rockville, MD) and was video recorded. The rotation angle of the filament was estimated from the centroid of the actin filament.
14. Immediately after the ATP addition, we rapidly scanned the 0.5-mm^2 area of a flow cell (containing <250 filaments) for 2 min. Under the standard assay conditions (*13*), we found at least one rotating filament in the cell. The following observations show that the rotating filaments were those connected to the c subunit: (i) The c subunit rotation could be observed in the presence of Triton X-100 but not in the absence of the detergent (0 rotating filaments out of 12,000). The addition of detergent may imitate the native lipid environment. In contrast, the γ subunit rotation in engineered F_1 was not dependent on the presence of the detergent. (ii) We isolated F_1 (no cysteine in the γ subunit, cysteine-less γ) from F_0F_1 (engineered for c subunit rotation) to test whether the actin filament can bind to the cysteine-less γ and rotate after the addition of ATP. We could find no rotating filaments (out of 10,000 filaments), which indicated that the contaminating F_1 (with cysteine-less γ), if any, is not responsible for the present results. (iii) SDS-polyacrylamide gel electrophoresis of the engineered F_0F_1 gave the same subunit ratio as that of previous reported preparations (*23*), indicating that the contamination of F_1 is minor. The rotation frequency of the filament directly connected to the F_1 γ subunit was slightly higher; about three filaments were observed when we rapidly scanned the area of ~0.5 mm^2 as described above.
15. Real-time video images of rotating filaments connected to the c subunit are available at www.sciencemag.org/feature/data/1045705.shl
16. P. C. Jones, W. Jiang, R. H. Fillingame, *J. Biol. Chem.* **273**, 17178 (1998); P. C. Jones and R. H. Fillingame, *J. Biol. Chem.* **273**, 29701 (1998); O. Y. Dmitriev, P. C. Jones, R. H. Fillingame, *Proc. Natl. Acad. Sci. U.S.A.* **96**, 7785 (1999).
17. D. S. Perlin, L. R. Latchney, A. E. Senior, *Biochim. Biophys. Acta* **807**, 238 (1985).
18. A pause was defined from the median filtered linear segment (as shown in Fig. 3A) as having coefficient of determination R^2 values of >0.96, a rotational rate between −0.2 and 0.2 rotations per second, and a dwell time of >67 ms.
19. We titrated the effects of venturicidin concentrations on the c subunit rotation and showing the results from 7 and 70 μM (Fig. 3B). The higher concentration was necessary for the inhibition under the rotation conditions. When we tested the effects of venturicidin in buffer A (*13*) containing 5 mM Mg ATP, 1 μM biotin, pyruvate kinase (50 μg/ml), 1 mM phosphoenol pyruvate, 25 mM glucose, 1% β-mercaptoethanol, glucose oxidase (216 μg/ml), and catalase (36 μg/ml), the inhibition of ATPase activity of F_0F_1 (purified or membranes) was ~10-fold lower than that reported previously (*20*). The weaker inhibitory effect was possibly due to the chemicals included in this study. The antibiotic was not inhibitory to the ATPase activity of F_1 under the same conditions.
20. R. H. Fillingame, M. Oldenburg, D. Fraga, *J. Biol. Chem.* **266**, 20934 (1991).
21. A. Iwamoto, J. Miki, M. Maeda, M. Futai, *J. Biol. Chem.* **265**, 5043 (1990); K. Shin, R. K. Nakamoto, M. Maeda, M. Futai, *J. Biol. Chem.* **267**, 20835 (1992); R. K. Nakamoto, M. Maeda, M. Futai; *J. Biol. Chem.* **268**, 867 (1993); R. K. Nakamoto, M. K. Al-Shawi, M. Futai, *J. Biol. Chem.* **270**, 14042 (1995); M. K. Al-Shawi, C. J. Ketchum, R. K. Nakamoto, *J. Biol. Chem.* **272**, 2300 (1997); C. Jeanteur–de Beukelar, H. Omote, A. Iwamoto-Kihara, M. Maeda, M. Futai, *J. Biol. Chem.* **270**, 22850 (1995).
22. A. D. Mehta, M. Rief, J. A. Spudich, D. A. Smith, R. M. Simmons, *Science* **283**, 1689 (1999).
23. Y. Moriyama, A. Iwamoto, H. Hanada, M. Maeda, M. Futai, *J. Biol. Chem.* **266**, 22141 (1991).
24. R. Yasuda, H. Noji, K. Kinoshita Jr., M. Yoshida, *Cell* **93**, 1117 (1998); A. J. Hunt, F. Gittes, J. Howard, *Biophys. J.* **67**, 766 (1994).
25. K. Svoboda, C. F. Schmidt, B. J. Schnapp, S. M. Block, *Nature* **365**, 721 (1993).

26. Supported in part by the Japanese Ministry of Education, Science, and Culture and by the Naito Foundation. We thank K. Saito and R. H. Fillingame for helpful discussions, M. A. Spies for critical reading of the manuscript, and N. Sambonmatsu for her technical assistance.

24 September 1999; accepted 28 October 1999

Visualization of Dioxygen Bound to Copper During Enzyme Catalysis

C. M. Wilmot,[1] J. Hajdu,[2] M. J. McPherson,[1] P. F. Knowles,[1] S. E. V. Phillips[1]

X-ray crystal structures of three species related to the oxidative half of the reaction of the copper-containing quinoprotein amine oxidase from *Escherichia coli* have been determined. Crystals were freeze-trapped either anaerobically or aerobically after exposure to substrate, and structures were determined to resolutions between 2.1 and 2.4 angstroms. The oxidation state of the quinone cofactor was investigated by single-crystal spectrophotometry. The structures reveal the site of bound dioxygen and the proton transfer pathways involved in oxygen reduction. The quinone cofactor is regenerated from the iminoquinone intermediate by hydrolysis involving Asp^{383}, the catalytic base in the reductive half-reaction. Product aldehyde inhibits the hydrolysis, making release of product the rate-determining step of the reaction in the crystal.

Oxygen is a ubiquitous electron acceptor in aerobic biological systems. The mechanisms of oxygen activation by redox enzymes, including *Escherichia coli* amine oxidase (ECAO), are poorly understood. To address this, we have used flash-freezing techniques on catalytically competent crystals of ECAO to trap intermediates in the oxidative half-reaction, and solve the

References and Notes

[5] **Rotation of Subunits During Catalysis by Escherichia coli F₁-ATPase**

Thomas M. Duncan; Vladimir V. Bulygin; Yuantai Zhou; Marcus L. Hutcheon; Richard L. Cross

Proceedings of the National Academy of Sciences of the United States of America, Vol. 92, No. 24. (Nov. 21, 1995), pp. 10964-10968.

Stable URL:

http://links.jstor.org/sici?sici=0027-8424%2819951121%2992%3A24%3C10964%3AROSDCB%3E2.0.CO%3B2-T

[7] **The γ-Subunit Rotation and Torque Generation in F ₁ -ATPase from Wild-Type or Uncoupled Mutant Escherichia coli**

Hiroshi Omote; Noriko Sambonmatsu; Kiwamu Saito; Yoshihiro Sambongi; Atsuko Iwamoto-Kihara; Toshio Yanagida; Yoh Wada; Masamitsu Futai

Proceedings of the National Academy of Sciences of the United States of America, Vol. 96, No. 14. (Jul. 16, 1999), pp. 7780-7784.

Stable URL:

http://links.jstor.org/sici?sici=0027-8424%2819990716%2996%3A14%3C7780%3ATRATGI%3E2.0.CO%3B2-5

[8] **Energy Transduction in the Sodium F-ATPase of Propionigenium modestum**

Peter Dimroth; Hongyun Wang; Michael Grabe; George Oster

Proceedings of the National Academy of Sciences of the United States of America, Vol. 96, No. 9. (Apr. 27, 1999), pp. 4924-4929.

Stable URL:

http://links.jstor.org/sici?sici=0027-8424%2819990427%2996%3A9%3C4924%3AETITSF%3E2.0.CO%3B2-W

LINKED CITATIONS

[22] **Single-Molecule Biomechanics with Optical Methods**
Amit D. Mehta; Matthias Rief; James A. Spudich; David A. Smith; Robert M. Simmons
Science, New Series, Vol. 283, No. 5408. (Mar. 12, 1999), pp. 1689-1695.
Stable URL:
http://links.jstor.org/sici?sici=0036-8075%2819990312%293%3A283%3A5408%3C1689%3ASBWOM%3E2.0.CO%3B2-%23